Entanglement-Controlled Subdiffusion of Nanoparticles within Concentrated Polymer Solutions

Hongyu Guo,[1] Gilles Bourret,[2] R. Bruce Lennox,[2] Mark Sutton,[3] James L. Harden,[4] and Robert L. Leheny[1]

[1]*Department of Physics and Astronomy, Johns Hopkins University, Baltimore, Maryland 21218, USA*
[2]*Department of Chemistry, McGill University, Montréal, Québec H3A 2K6, Canada*
[3]*Department of Physics, McGill University, Montréal, Québec H3A 2K6, Canada*
[4]*Department of Physics, University of Ottawa, Ottawa, Ontario K1N 6N5, Canada*

(Received 15 March 2012; published 2 August 2012)

We describe x-ray photon correlation spectroscopy (XPCS) experiments tracking the motion of gold nanoparticles within solutions of high-molecular-weight polystyrene. Over displacements from nanometers to tens of nanometers, the particles undergo subdiffusive motion that is dictated by the temporal evolution of the entangled polymer mesh in the immediate vicinity of the particles. The results thus provide a novel microscopic dynamical characterization of this key structural property of polymers and more broadly demonstrate the capability of XPCS-based microrheology to interrogate heterogeneous mechanical environments in nanostructured soft materials.

DOI: 10.1103/PhysRevLett.109.055901 PACS numbers: 83.80.Rs, 66.10.cg, 66.30.hk, 83.85.Hf

Complex fluids—such as polymer and surfactant solutions—are characterized by internal structure on the nanometer or micrometer scale that creates complicated viscoelastic behavior. Due to the microscopic heterogeneity of these systems, the relation between macroscopic mechanical properties and microscopic structure and dynamics is rarely straightforward. Microrheology, in which colloids suspended in the fluid probe the mechanical environment, has emerged as a technique capable of illuminating this connection. Traditionally, microrheology has employed colloids that are much larger than the scale of the intrinsic heterogeneity of the complex fluid, so that Brownian motion of the probes reflects the material's macroscopic viscoelastic properties [1]. However, if the probe size is comparable to or smaller than the scale of the heterogeneity, the correspondence with macroscopic rheology breaks down [2], leading to alternative information about the microstructure and micromechanics that might otherwise be inaccessible. This feature of microrheology has been demonstrated in several microscopy and dynamic light scattering (DLS) studies [2–9]. For example, experiments on networks of the semiflexible biopolymer F-actin have tracked changes in the mobility of micrometer-sized colloids as the colloid size is varied with respect to the network mesh size [7,9].

In many important complex fluids the scale of the relevant internal structure is well below the micrometer scale. For example, in solutions of high-molecular-weight flexible polymers, the relevant entities are chain entanglements. The characteristic lengths of this microstructure that emerge from models of entanglements are typically on the nanometer scale, and the time scales characterizing their dynamics can extend to many seconds. While such models account successfully for various macroscopic properties of polymer melts and solutions [10], such as scaling behavior of the rheology, this challenging combination of length and time scales has permitted few direct microscopic investigations of entanglement behavior [11–15]. Here, we report an x-ray photon correlation spectroscopy (XPCS) study of nanoparticle motion within solutions of high-molecular-weight polystyrene (PS) in which we tune the particle size to the length scales relevant to entanglements, thus providing a local microrheological viewpoint. The particle motion is subdiffusive with a mean-squared displacement that grows as $\langle \Delta r^2(t) \rangle \sim t^{\alpha}$ with $\alpha = 0.27$ to 0.53 depending on solution parameters. Studies of particle motion within crowded macromolecular environments have observed similar subdiffusion [16–20], but the underlying mechanisms for this behavior are as yet unclear. By varying polymer molecular weight and comparing the XPCS results with macroscopic rheology, we conclude that the subdiffusive motion in the high-molecular-weight solutions is dictated by fluctuations of the entanglement mesh within the local environment of the nanoparticles.

The systems were solutions of PS in xylene containing dilute dispersions of Au nanoparticles with concentration 0.04% Au by volume. The nanoparticles, with radius ≈ 3 nm, were synthesized following procedures described elsewhere [21]. To stabilize the particles, their surfaces were functionalized with thiol-terminated PS chains with molecular weight 13 300 g/mol [21,22]. The resulting hydrodynamic radius of the particles was approximately 20 nm [22]. Solutions with PS molecular weights from $M_w = 3 \times 10^5$ g/mol to 9×10^6 g/mol and polymer volume fractions from $\phi = 0.1$ to 0.4 were included in the study.

Rheometry on the solutions over frequencies $0.001\ \mathrm{s}^{-1} < \omega < 100\ \mathrm{s}^{-1}$ revealed complex shear moduli, $G^*(\omega) = G'(\omega) + iG''(\omega)$, typical of entangled polymers. Figure 1 shows the storage and loss modulus at two temperatures for $M_w = 1 \times 10^6$ g/mol and $\phi = 0.3$. The form of $G^*(\omega)$ and its temperature dependence are

representative of all the solutions. At intermediate frequencies, $G'(\omega)$ is approximately constant and $G'(\omega) > G''(\omega)$. This plateau is associated with a transient rubbery response due to the mesh of entanglements, and the plateau value G_e can be related to the entanglement density, $G_e = k_B T/L^3$, where L^3 is the volume per entanglement [23]. In terms of lengths commonly discussed in models of entanglements, the tube diameter a and correlation length ξ, $L^3 = a^2\xi$. From measurements of each solution's plateau modulus, we obtained values of L in the range $5 < L < 20$ nm, with L increasing with decreasing ϕ as expected. We note that L, which represents a typical distance between entanglements, is similar to the nanoparticle hydrodynamic radius, indicating a match between the scale of the transient network structure dictating the solution rheology and the probe size.

At low frequencies, the solutions are fluid with $G''(\omega) > G'(\omega)$ and $G''(\omega) \sim \omega$ and with zero-shear-rate viscosity $\eta_0 = \lim_{\omega\to 0} G''(\omega)/\omega$. We identify the reptation time $t_{\rm rep}$ [23] as the inverse of the frequency $\omega_{\rm rep}$ where $G''(\omega_{\rm rep})/G'(\omega_{\rm rep}) = 1$. For example, from Fig. 1, we obtain reptation times for $M_w = 1 \times 10^6$ g/mol and $\phi = 0.3$ of $t_{\rm rep} = 6.3$ s and 0.083 s at $-5\,^\circ$C and $50\,^\circ$C, respectively. Within models of entanglements, $t_{\rm rep}$ is the time for entanglements along a chain to relax [23].

To track the nanoparticle motion, we employ XPCS. Experiments were conducted at Sector 8-ID of the Advanced Photon Source using 7.35 keV x rays following established procedures [24]. Samples were contained in sealed stainless-steel holders with sample thickness 2 mm and with kapton windows for transmission scattering. The coherent scattering intensity, recorded by a direct-illuminated CCD area detector, was measured over wave vectors $0.04\ {\rm nm}^{-1} < Q < 0.21\ {\rm nm}^{-1}$. Time-resolved series of scattering intensities were analyzed to determine the intensity time-autocorrelation function $g_2(Q, t)$ over delay times $0.0167\ {\rm s} < t < 1000$ s. Scattering from the Au dominates the signal in this Q range, and the intensity resembles the form factor for an isolated particle [22].

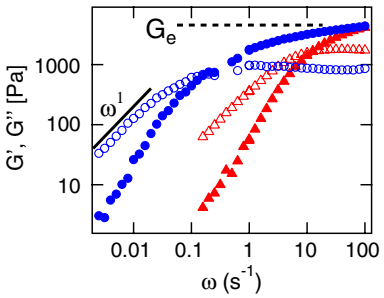

FIG. 1 (color online). Storage (solid) and loss (open) modulus of PS in xylene with $M_w = 1 \times 10^6$ g/mol and $\phi = 0.3$ containing a dilute concentration of Au nanoparticles at $T = -5\,^\circ$C (circles) and $50\,^\circ$C (triangles). The dashed line indicates the plateau modulus.

Thus, $g_2(Q, t)$ reflects the dynamics of the dilute nanoparticle suspension. Following a temperature change, measurements were performed only after any transient effects vanished, so that $g_2(Q, t)$ corresponded to nanoparticle motion within equilibrated, quiescent solutions.

Figure 2 displays $g_2(Q, t)$ for $M_w = 1 \times 10^6$ g/mol and $\phi = 0.3$ at $T = -20\,^\circ$C and $Q = 0.09\ {\rm nm}^{-1}$. The solid line through the data is the result of a fit to a stretched-exponential form,

$$g_2(Q, t) = 1 + b g_1^2(Q, t) = 1 + b\{\exp[-2(t/\tau_{\rm SE})^\alpha]\}, \quad (1)$$

where b is the Siegert factor and $g_1(Q, t)$ is the normalized dynamic structure factor. The exponent α is significantly less than one for all solutions (e.g., in Fig. 2, $\alpha = 0.45 \pm 0.05$), indicating a highly stretched decay. The exponent shows no systematic dependence on T or Q over the full experimental ranges ($-20\,^\circ{\rm C} < T < 50\,^\circ{\rm C}$ and $0.04\ {\rm nm}^{-1} < Q < 0.21\ {\rm nm}^{-1}$). However, as shown in the inset to Fig. 2, α does vary with polymer molecular weight. We discuss the possible significance of this variation below. Figure 3 displays the mean XPCS relaxation time $\tau = \tau_{\rm SE}\Gamma(\alpha^{-1})/\alpha$, where Γ denotes the gamma function, scaled by solution viscosity η_0 as a function of Q for $M_w = 1 \times 10^6$ g/mol at different T and ϕ. As the results indicate, the mean XPCS relaxation time varies with Q as a strong power law, $\tau \sim Q^{-p}$. ($p \approx 4$ in Fig. 3.) Similar power-law behavior is observed for all solutions with p varying weakly with M_w.

For dilute, noninteracting particles, $g_1(Q, t)$ is related to the particles' mean-squared displacement $\langle\Delta r^2(t)\rangle$ through $g_1(Q, t) = \exp(-\langle\Delta r^2(t)\rangle Q^2/6)$, which by Eq. (1) leads to $p\alpha = 2$ and $\langle\Delta r^2(t)\rangle \sim t^\alpha$. Thus, the stretched-exponential correlation functions, $\alpha < 1$, imply anomalous, subdiffusive motion. For most solutions, $p\alpha = 2$ within experimental uncertainty at all T. From the signal to noise in

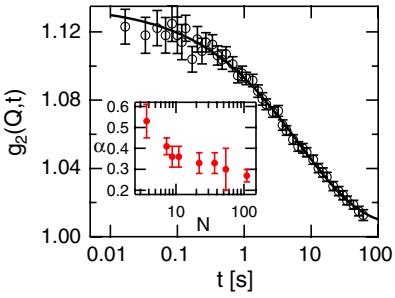

FIG. 2 (color online). XPCS intensity autocorrelation function for PS solution with $M_w = 1 \times 10^6$ g/mol and $\phi = 0.30$ containing a dilute concentration of Au nanoparticles at $T = -20\,^\circ$C and $Q = 0.09\ {\rm nm}^{-1}$. The line is the result of a fit to a stretched-exponential form, Eq. (1), with exponent $\alpha = 0.45 \pm 0.05$ characterizing the subdiffusive nanoparticle motion. The inset shows α for different solutions as a function of the number of entanglements per chain, $N = M_w\phi^{-1.3}/M_e(1)$, where $M_e(1) = 17\,000$ g/mol is the entanglement molecular weight of PS melt [10].

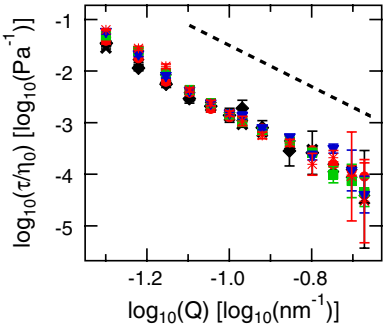

FIG. 3 (color online). Mean XPCS relaxation times normalized by solution viscosity as a function of wave vector for solutions with $M_w = 1 \times 10^6$ g/mol and $\phi = 0.3$ at $T = -20\,^\circ$C (red circles), $\phi = 0.3$ at $T = -5\,^\circ$C (black $\times$s), $\phi = 0.3$ at $T = 10\,^\circ$C (green squares), $\phi = 0.3$ at $T = 25\,^\circ$C (blue inverted triangles), $\phi = 0.3$ at $T = 50\,^\circ$C (red stars), and $\phi = 0.2$ at $T = 25\,^\circ$C (black diamonds). The dashed line displays the relation $\tau \sim Q^{-4}$.

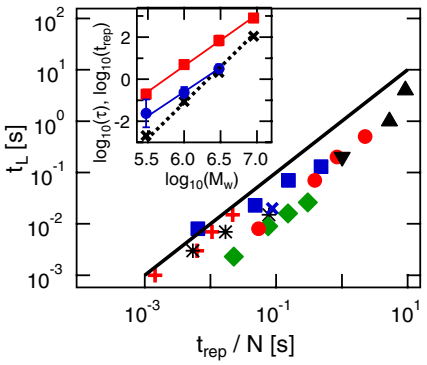

FIG. 4 (color online). Average time t_L for nanoparticles to move the entanglement spacing L as a function of $t_{\rm rep}/N$, where $t_{\rm rep}$ is the reptation time obtained from rheology and N is the entanglements per chain. Included are data for all solutions and T for which both t_L and $t_{\rm rep}$ are determined accurately: $M_w = 3 \times 10^5$ g/mol and $\phi = 0.3$ (stars), 1×10^6 g/mol and 0.2 (pluses), 1×10^6 g/mol and 0.3 (squares), 3×10^6 g/mol and 0.1 ($\times$ s), 3×10^6 g/mol and 0.2 (diamonds), 3×10^6 g/mol and 0.3 (circles), 3×10^6 g/mol and 0.4 (triangles), and 9×10^6 g/mol and 0.3 (inverted triangles). The line shows the relation $t_L = t_{\rm rep}/N$. Inset: mean XPCS relaxation time at 25 °C and $Q = 0.09$ nm^{-1} versus PS molecular weight for solutions with $\phi = 0.3$ (squares) and 0.2 (circles) along with the results of power-law fits $\tau \sim M_W^{2.4\pm0.1}$ (solid lines). Also in the inset are the reptation times ($\times$ s) for $\phi = 0.3$ at 50 °C along with the result of a power-law fit, $t_{\rm rep} \sim M_w^{3.2\pm0.2}$ (dashed line).

$g_2(Q, t)$ and the accuracy of the stretched-exponential fits over the measurement wave vectors, we estimate that this subdiffusive motion extends at least over root-mean-squared displacements of $6\ \text{nm} < \langle \Delta r^2(t) \rangle^{1/2} < 50\ \text{nm}$. That is, the subdiffusion extends to several times the entanglement spacing L.

To understand the nature of this subdiffusive nanoparticle motion and its connection with the viscoelastic environment in the solutions, we compare the particle dynamics with the solution rheology. In Fig. 3 the mean XPCS relaxation times are scaled by solution viscosity η_0, which varies at the different ϕ and T by more than a factor of 300. Nevertheless, the scaled relaxation times collapse, indicating the nanoparticle motion depends on the same microscopic friction factor [10] that enters the chain mobility.

A more surprising feature of the nanoparticle mobility is its dependence on polymer molecular weight. The inset to Fig. 4 shows τ at 25 °C and $Q = 0.09$ nm^{-1} as a function of M_w for $\phi = 0.2$ and 0.3. As the figure illustrates, $\tau \sim M_w^{2.4}$. This strong dependence indicates that entanglements play an important role in dictating the nanoparticle motion. However, consistent with expectations for highly entangled solutions [23], we find $\eta_0 \sim M_w^z$ where $z = 3.2 \pm 0.2$. Thus, the particle mobility does not scale with the macroscopic viscosity as polymer molecular weight is varied, as one would expect for the diffusivity of a larger colloid. Rather, the trend in the inset to Fig. 4 marks a deviation of the subdiffusive nanoparticle motion from the macroscopic properties of the solutions that we associate with the similarity between the nanoparticle size and L. Indeed, XPCS experiments with the nanoparticles in PS melts, where L is smaller, observed simple diffusion [25].

Recently, Rubinstein and coworkers considered theoretically the mobility of nanoparticles in entangled polymers [26]. Particles significantly larger than the entanglement mesh were found to undergo simple diffusion with a rate set by the reptation time, which is proportional to the macroscopic viscosity. However, for particles that were similar to the mesh size, they identified an additional contribution to the mobility due to local fluctuations of the mesh that allow particles to pass through ''entanglement gates'' and hop between neighboring entanglement cages [26]. While the authors did not make explicit predictions about the consequences of this mechanism, we hypothesize that such fluctuation-enabled hopping dictates the observed subdiffusive motion.

Within this picture, the scaling of particle mobility with molecular weight, $\eta_0 \sim M_w^{2.4}$, indicates that such fluctuations become increasingly important the more highly entangled the solution. Specifically, models of entanglement relaxation predict $t_{\rm rep} \sim M_w^{3.4}$ [10], and as illustrated in the inset to Fig. 4, our results for $t_{\rm rep}$ are consistent with this scaling. Meanwhile, the number of entanglements N along a chain varies as $N = M_w/M_e(\phi) = M_w \phi^{-1.3}/M_e(1)$ where $M_e(1) = 17\,000$ g/mol is the entanglement molecular weight of PS melt [10]. Together, these relationships suggest $\tau \sim t_{\rm rep}/N$. Thus, particle mobility is enhanced over that expected from macroscopic rheology linearly with the degree of entanglement.

To analyze this enhancement more quantitatively, we identify an average time t_L for particles to hop between neighboring entanglement cages. We determine t_L from $g_2(Q, t)$ as the time the particles' root-mean-squared

displacement reaches L, $\langle \Delta r^2(t_L) \rangle^{1/2} = L$. Figure 4 displays t_L plotted against t_{rep}/N. Included in the figure are data corresponding to all the solutions in the study at all T for which we are able to determine accurately both t_L and t_{rep}. The data collapse onto a linear relation between t_L and t_{rep}/N with a proportionality constant that is remarkably close to unity. (A linear best fit gives $t_L = 0.3 t_{\mathrm{rep}}/N$.)

This near equality between t_L and t_{rep}/N demonstrates the central role of entanglements in dictating the nanoparticle mobility. Support for this conclusion also comes from the range of length scales over which the XPCS measurements track the motion. As mentioned above, this length extends over distances of several L, thereby precluding a significant role in the observed mobility for other, more local relaxation modes in the solutions. For example, in a previous DLS study of colloids bound to polymer networks, the authors attributed localized subdiffusive motion at short time scales ($t < 1$ ms) to Rouse dynamics [27,28]. While Rouse-like dynamics seems a natural explanation for the observed motion of the bound colloids in that study, in the PS solutions in our study, the relaxation times of Rouse modes with wavelengths near the entanglement spacings are in the millisecond range and therefore significantly shorter than the XPCS relaxation times. Thus, Rouse modes should fully relax on time scales that are much shorter than those characterizing the nanoparticle motion. Further, the model of Rouse dynamics predicts motion that is independent of matrix molecular weight [27,28], in stark contrast to the trend in the inset to Fig. 4.

The mechanism of fluctuation-enabled hopping through the entanglement mesh [26] also provides an explanation for the subdiffusive nature of the motion. Anomalous diffusion, characterized by power-law mean-squared displacements with $\alpha \neq 1$, appears in many contexts in nature [29]. A possible source of subdiffusion is the persistence of negative correlations in the steps by objects undergoing Brownian motion [30,31]. In the motion of a nanoparticle in an entangled solution, a cause for negative correlations is suggested by the proposed entanglement fluctuations. If such fluctuations are sufficiently long-lived, the most probable direction of motion for a nanoparticle that passes through an entanglement gate is back to its previous position, and this enhanced probability should decay with time as the fluctuation decays. The degree of subdiffusion, which is expressed in the exponent α, and any possible crossover to normal diffusion at late times hence convey information about the temporal form of this time-dependent preference. As indicated in the inset to Fig. 2, α depends on the number of entanglements per chain N in a manner that makes the motion increasingly subdiffusive with increasing N, consistent with the notion that negative correlations are enhanced in more strongly constrained environments. This observation to our knowledge cannot be explained easily within existing mean-field models of entanglement formation and relaxation [10,23]. It would be interesting to see if a fully developed theory for nanoparticle motion that incorporates the proposed hopping mechanism due to heterogeneous fluctuations in the entanglement mesh [26] can capture the behavior. More broadly, these findings demonstrate the strong potential of XPCS as a microrheological technique for interrogating the local mechanical properties of soft materials. The wealth of important complex fluids with nanometer-scale heterogeneity that are amenable to this approach should make further application of XPCS to microrheology an important new tool for this field of research.

We thank M. Shlesinger for helpful discussions and S. Narayanan and A. Sandy for their expert assistance. Funding was provided by the Petroleum Research Fund and NSERC. Use of the APS was supported by DOE BES under Contract No. DE-AC02-06CH11357.

[1] T. G. Mason, Rheol. Acta **39**, 371 (2000).
[2] Q. Lu and M. J. Solomon, Phys. Rev. E **66**, 061504 (2002).
[3] F. Amblard, A. C. Maggs, B. Yurke, A. N. Pargellis, and S. Leibler, Phys. Rev. Lett. **77**, 4470 (1996).
[4] S. Köster, Y.-C. Lin, H. Herrmann, and D. A. Weitz, Soft Matter **6**, 1910 (2010).
[5] M. A. Kotlarchyk, E. L. Botvinick, and A. J. Putman, J. Phys. Condens. Matter **22**, 194121 (2010).
[6] F. K. Oppong and J. R. de Bruyn, Eur. Phys. J. E **31**, 25 (2010).
[7] J. H. Shin, M. L. Gardel, L. Mahadevan, P. Matsudaira, and D. A. Weitz, Proc. Natl. Acad. Sci. U.S.A. **101**, 9636 (2004).
[8] M. T. Valentine, P. D. Kaplan, D. Thota, J. C. Crocker, T. Gisler, R. K. Prud'homme, M. Beck, and D. A. Weitz, Phys. Rev. E **64**, 061506 (2001).
[9] I. Y. Wong, M. L. Gardel, D. R. Reichman, E. R. Weeks, M. T. Valentine, A. R. Bausch, and D. A. Weitz, Phys. Rev. Lett. **92**, 178101 (2004).
[10] M. Rubinstein and R. H. Colby, *Polymer Physics* (Oxford, New York, 2003).
[11] T. T. Perkins, D. E. Smith, and S. Chu, Science **264**, 819 (1994).
[12] F. Vaca Chávez and K. Saalwächter, Phys. Rev. Lett. **104**, 198305 (2010).
[13] D. Lumma, M. A. Borthwick, P. Falus, L. B. Lurio, and S. G. J. Mochrie, Phys. Rev. Lett. **86**, 2042 (2001).
[14] D. Richter, B. Farago, R. Butera, L. J. Fetters, J. S. Huang, and B. Ewen, Macromolecules **26**, 795 (1993).
[15] D. Wöll, E. Braeken, A. Deres, F. C. D. Schryver, H. Uji-i, and J. Hofkens, Chem. Soc. Rev. **38**, 313 (2009).
[16] D. S. Banks and C. Fradin, Biophys. J. **89**, 2960 (2005).
[17] I. Golding and E. C. Cox, Phys. Rev. Lett. **96**, 098102 (2006).
[18] G. Guigas, C. Kalla, and M. Weiss, Biophys. J. **93**, 316 (2007).
[19] R. A. Omari, A. M. Aneese, C. A. Grabowski, and A. Mukhopadhyay, J. Phys. Chem. B **113**, 8449 (2009).
[20] I. M. Tolić-Norrelykke, E.-L. Munteanu, G. Thon, L. Oddershede, and K. Berg-Sorensen, Phys. Rev. Lett. **93**, 078102 (2004).

[21] M. K. Corbierre, N. S. Cameron, M. Sutton, S. G. J. Mochrie, L. B. Lurio, A. Ruhm, and R. B. Lennox, J. Am. Chem. Soc. **123**, 10411 (2001).
[22] M. K. Corbierre, N. S. Cameron, M. Sutton, K. Laaziri, and R. B. Lennox, Langmuir **21**, 6063 (2005).
[23] M. Doi and S. F. Edwards, *The Theory of Polymer Dynamics* (Oxford, New York, 1988).
[24] D. Lumma, L. B. Lurio, S. G. J. Mochrie, and M. Sutton, Rev. Sci. Instrum. **71**, 3274 (2000).
[25] H. Guo, G. Bourret, M. K. Corbierre, S. Rucareanu, R. B. Lennox, K. Laaziri, L. Piche, M. Sutton, J. L. Harden, and R. L. Leheny, Phys. Rev. Lett. **102**, 075702 (2009).
[26] L.-H. Cai, S. Panyukov, and M. Rubinstein, Macromolecules **44**, 7853 (2011).
[27] J. Sprakel, J. van der Gucht, M. A. Cohen Stuart, and N. A. M. Besseling, Phys. Rev. Lett. **99**, 208301 (2007).
[28] J. Sprakel, J. van der Gucht, M. A. Cohen Stuart, and N. A. M. Besseling, Phys. Rev. E **77**, 061502 (2008).
[29] *Anomalous Transport* R. Klages, G. Radons, and I. M. Sokolov (Wiley, New York, 2008).
[30] J.-P. Bouchaud and A. Georges, Phys. Rep. **195**, 127 (1990).
[31] K. W. Kehr, R. Kutner, and K. Binder, Phys. Rev. B **23**, 4931 (1981).